The Multiplicity, Strength, and Nature of the Interaction of Nucleobases with Alkaline and Alkaline Earth Metal Cations: A Density Functional Theory Investigation

Weiliang Zhu,[†,‡,§] Xiaomin Luo,[‡] Chum Mok Puah,[*,§] Xiaojian Tan,[‡] Jianhua Shen,[‡] Jiande Gu,[‡] Kaixian Chen,[‡] and Hualiang Jiang[*,‡,⊥]

School of Chemical and Life Sciences, Singapore Polytechnic, 500 Dover Road, Singapore 139651, Centre for Drug Discovery and Design, State Key Laboratory of Drug Research, Shanghai Institute of Materia Medica, Shanghai Institutes for Biological Sciences, Chinese Academy of Sciences, 555 Zuchongzhi Road, Shanghai 201203, P. R. China, and Technology Centre for Life Sciences, Singapore Polytechnic, 500 Dover Road, Singapore 139651

Received: September 29, 2003; In Final Form: December 22, 2003

Density functional theory (DFT) calculations were performed at the B3LYP/6-311++G(d,p) level to systematically explore the geometrical multiplicity and binding strength for the complexes formed by alkaline and alkaline earth metal cations, viz. Li^+, Na^+, K^+, Be^{2+}, Mg^{2+}, and Ca^{2+} (M^{n+}, hereinafter), with nucleobases, namely, adenine, cytosine, guanine, thymine, and uracil. Morokuma decomposition and orbital analysis were used to analyze the binding components. A total of 150 initial structures were designed and optimized, of which 93 optimized structures were found, which could be divided into two different types: cation−π complex and cation−heteroatom complex. In the former, a M^{n+} is located above the nucleobase ring, while in the latter a M^{n+} directly interacts in flank with the heteroatom(s) of a nucleobase. The strongest binding of −319.2 kcal/mol was found in the Be^{2+}−guanine complex. Furthermore, the planar ring structures of the nucleobases in some cation−π complexes were deformed, destroying more or less the aromaticity of the corresponding nucleobases. In the cation−heteroatom complex, bidentate binding is generally stronger than unidentate binding, and of which the bidentate binding with five-membered ring structure has the strongest interaction. Moreover, the calculated Mulliken charges showed that the transferred charge is linearly proportional to the binding strength. Molecular orbital coefficient analysis indicated a significant orbital interaction in cation−π complex, but not in cation−heteroatom interaction. In addition, Morokuma decomposition revealed that electrostatic interaction is more important for cation−heteroatom binding. The majority of the calculated ΔH values are in good agreement with the experimental results. In those cases with significant differences, the experimental results are proximate to an average of the ΔH values of two isomers formed by the same nucleobase and cation.

1. Introduction

Great efforts have been made in the past three decades in the field of intermolecular interaction. Results accumulated to date showed that this noncovalent interaction plays a dominant role in many scientific areas.[1] For instance metal ions are almost involved in almost all biological processes, such as the regulation of enzyme, stabilization, and function of nucleic acids. Thus, the role of metal ions in the structures and functions of proteins, nucleic acids, and peptide hormones is of fundament significance. However, the understanding behind this interaction remains elusive, especially in nucleic acids at both electronic and atomic levels.[2−4] Therefore, further investigations on how metal cations interact with biological molecules and how these interactions affect, adjust, or control the functions of biological molecules are essential for better understanding of the role and effect of metal ions in biological systems. Of special interest to us are the alkaline and alkaline earth metal cations, e.g., Na^+, K^+, Mg^{2+}, and Ca^{2+}, which prevail in almost all organisms, known to be involved in many important biological functions. For example, the synthesis, replication, and cleavage of DNA and RNA, as well as their structural integrity, are somewhat affected by these cations in either free or protein-bound forms. Furthermore, high concentrations of metal ions may interact with the nucleobases, leading to the disruption of the base pair hydrogen bonding, thus compromising the structural integrity of the nucleic acid polymer.[3−4]

In general, direct investigation on the interactions of the M^{n+} with nucleic acids, at either experimental or theoretical levels, was found to be tedious and time consuming. However, knowledge about an intrinsic binding model can significantly enhance our understanding of how these metal cations play their roles in living systems. In fact, in the 1980s some investigations were carried out on small model systems, involving some calculations on the interactions between metal cations and either bases or base pairs.[5−7] Although they were usually carried out at low theoretical levels, such as semiempirical or Hartree−Fock approximations, they did provide some useful information on how metal ions interact with nucleobases.[5−9] Recently, Šponer and co-workers calculated the structures and energetics of the complexes of nucleobases or base pairs with mono- or divalent metal cations at HF/6-31G* and MP2/6-31G* levels.[10−11]

* Address correspondence to this author.
† School of Chemical and Life Sciences, Singapore Polytechnic.
‡ Shanghai Institutes for Biological Sciences.
§ Technology Centre for Life Sciences, Singapore Polytechnic.
⊥ Phone +86-21-50807188. Fax: +86-21-50807088. E-mail: hljiang@mail.shcnc.ac.cn or jiang@iris3.simm.ac.cn.

10.1021/jp036911n CCC: $27.50
Published on Web 04/14/2004

Hoyau and co-workers carried out high-pressure mass spectrometric (HPMS) studies and ab initio calculations at the MP2/6-311+G(2df,2pd)//MP2/6-31G* level on the binding of Na^+ with nucleobases.[12] Cerda's group determined the affinities of group Ia cations with nucleobases by investigating the dissociation of cation-bound heterodimers.[13] They also calculated the binding strength of Na^+ to nucleobases at the MP2/6-311+G-(2df,2pd) level by using HF/6-31G* geometries.[13] Burda and co-workers calculated the interactions of guanine and adenine with 15 ions of groups Ia, Ib, IIa, and IIb at the Hartree−Fock and the second-order Møller−Plesset levels.[14] However, they limited geometrical optimization to the planar C_s structures of the base···X^{n+} complexes, where the metal cations X^{n+} interact with the nitrogen atom N7 of adenine or N7 and O6 atoms of guanine. Also, they employed the 6-31G** basis set for guanine and adenine, and the DZ basis set of Schaefer for metal cations. In another study, Russo and co-workers performed B3LYP/6-311+G(2df,2p) calculations on the interactions of alkali cations (Li^+, Na^+, and K^+) with DNA and RNA nucleic bases.[15,16] They calculated the binding affinity between M^+ and all possible tautomers of DNA and RNA nucleic bases. Interestingly, their results are in good agreement with most of the experimental results. Although all this research released a considerable amount of information, it also showed that a significant number of data that were published earlier required intensive revision, which, therefore, calls for a systematic investigation. On the other hand, due to the special planar ring structure of nucleobases, it is valuable to emphasize the capability of the nucleobases to bind to metal cations to form both cation−π-like and hydrogen-bonding-like complexes. However, to the best of our knowledge, no systematic investigation on the binding of alkali and alkaline earth metal cations to nucleobases, taking into account the potential cation−π interaction, has been published.

Current force fields are supposed to be capable of handling macromolecules. Unfortunately, they fail to account adequately for some special noncovalent interactions, such as cation−π interaction that was found prevalently in biological system. However, the modification of current force fields with some parameters from quantum chemistry calculations might be a feasible way to reproduce this special kind of interaction.[17] Therefore, systematic quantum chemistry calculation on the interaction between nucleobases and metal cations might provide more useful geometrical and energetic data for further improvement of current force fields.

Density functional theory[18] (DFT) has recently been widely recognized as an efficient quantum chemistry method for studying molecular properties. DFT with the B3LYP functional[19] has shown its reliability in predicting the geometries, binding energies, and frequencies of metal cation−π or metal cation−heteroatom complexes with fewer computer resources in comparison with other quantum chemistry methods such as MP2.[20−21] Furthermore, the published calculation results demonstrated that the basis set 6-311++G(d,p) is large enough to generally reduce the basis set superposition error (BSSE) to ~1 kcal/mol.[22−24] Therefore, the B3LYP/6-311++G(d,p) method was used in this study and the BSSE correction was not taken into account.

The nucleobases included in this study are adenine, guanine, cytosine, thymine, and uracil. In addition to these five nucleobases, pyridine and imidazole are also included, to compare the difference, if any, between nucleobases and heterocyclics of their bindings with the M^{n+}. Morokuma analysis was carried out at the HF/6-31G** level.[25] The objectives of this study are (a) to study the multiplicity of the binding between the M^{n+} and the nucleobases, (b) to find the most probable geometries of the M^{n+}−nucleobase complexes, (c) to explore their binding strength and nature, and (d) to provide geometrical and thermodynamic parameters for modifying current force fields. In this study, we also included the alkali metal cations, for we are interested in both hydrogen-bonding-like bindings of M^{n+} to all potential binding sites and possible cation−π interactions.

2. Computational Details

To probe all possible binding sites, 150 initial structures were designed for geometrical optimization (Figure 1). These initial structures could be divided into two groups. One is cation−heteroatom complex, in which a M^{n+}, lying in the same plane as the ring structure of a nucleobase, interacts directly by flanking the heteroatom. The other is the cation−π complex, whereby a M^{n+} is located above the nucleobase ring and is supposed to interact with all ring atoms of a nucleobase. All these 150 initial structures were fully optimized at the B3LYP/6-31G* level, followed by a B3LYP/6-311++G(d,p) optimization and frequency calculations, to predict their entropies, enthalpies, and free energies. The thermal energy and zero-point vibratonal energy (ZPVE) were taken into account during the calculation of binding energy, enthalpy, and free energy. All the calculations were performed by using the software G98(W).[26] The Morokuma analyses were carried out at the HF/6-31G** level based on HF/6-31G** geometries with the software Gamess.[27]

3. Results and Discussions

3.1. Cation−π Complexes. Figure 2 depicts the 17 optimized cation−π structures generated from the geometrical optimizations of the 54 initial cation−π structures. In total there are four cations, viz. Li^+, Be^{2+}, Mg^{2+}, and Ca^{2+}, that are capable of forming cation−π complexes with nucleobases, of which Be^{2+} can form cation−π complexes with all nucleobases except guanine. Regarding guanine, only one stable cation−π structure was obtained, which is the guanine−Li^+ complex shown in Figure 2f. Other initial cation−π structures of cation−guanine complexes underwent either an opened-ring change or a geometrical conversion to cation−heteroatom complexes during the geometry optimization. All the geometrical optimization results did not show the capability of the cation−π binding of nucleobases with either Na^+ or K^+.

Although the optimized structures clearly show a distortion of the nucleobase planar ring structures, the degree of distortion varied among the different complexes. Table 1 summarized the torsion, $T_{1-2-3-4}$ (refer to Figure 2 for the atomic numbering). The $T_{1-2-3-4}$ for adenine and guanine complexes ranged from 154° to 175°. But, in cytosine, thymine, and uracil complexes, the torsions are always less than 150°, far from a planar structure. Therefore, adenine and guanine have stronger capabilities to maintain their planar ring structures in their cation−π complexes in comparison with cytosine, thymine, and uracil. To quantitatively explore how serious the distortion is, the distortion energy, E_d, was estimated at the B3LYP/6-311++G-(d,p) level, which is defined as the energy difference between the structure extracted directly from its optimized cation−π structure and the corresponding free nucleobase (Table 1). The E_d of cytosine, thymine, and uracil could be as high as 51 kcal/mol, demonstrating that the aromaticity of these three nucleobases could almost be destroyed, especially in their Be^{2+}−π or Mg^{2+}−π complexes. Subsequently, we like to refer to these complexes as "cation−π-like" complexes. While adenine and

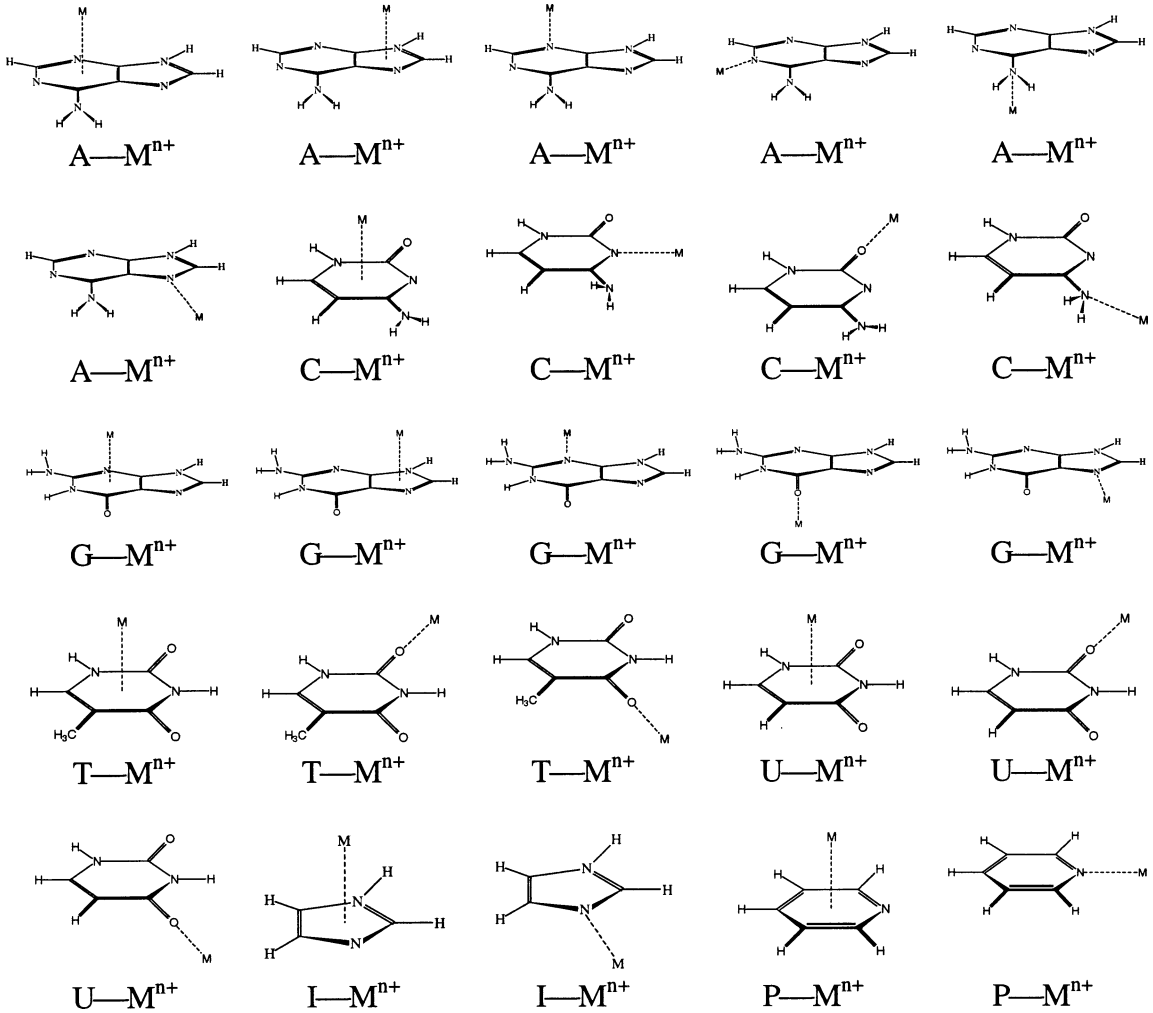

Figure 1. The 150 initial structures formed by metal cations with nucleobases. A, C, G, T, U, I and P represent nucleobases adenine, cytosine, guanine, thymine, uracil and heterocyclics imidazole and pyridine, respectively. M^{n+} stands for alkaline or alkaline earth metal cations Li^+, Na^+, K^+, Be^{2+}, Mg^{2+} and Ca^{2+}, respectively. Ninety-six of these 150 initial structures are cation−heteroatom complex, and the other 54 are cation−π complex.

guanine have a condensed-ring structure, cytosine, thymine, and uracil do not, indicating that the condensed ring structure has a stronger capability to keep its planar structure in its cation−π complex. On the other hand the radius and charge of a cation can affect the distortion notably. Hence, the smaller the ion radius and the more positive its charge, the larger the ring distortion.

Although the two heterocyclics, imidazole and pyridine, are also of mono-ring structures, they are still capable of retaining their planar structures in their cation−π complexes with the $T_{1-2-3-4}$ ranging from 173° to 177°. The difference between these two common heterocyclics and the nucleobases is that common heterocyclics have no carbonyl (C═O) structural unit, suggesting that the existence of the C═O unit in the nucleobases results in significant distortion of the nucleobase ring structure during the cation−π complexation. Furthermore, there is no distortion of the planar ring structure of benzene in all its cation−π complexes.[28] It is interesting to note that the significant distortion of the nucleobase planar structures might weaken or break the hydrogen bonding in base pairs, thereby affecting the function of the corresponding nuclear acid codes.

The perpendicular interaction distances, *R*, between the cations and nucleobase rings are also listed in Table 1 (refer to Figure 2 for the distances). It was found that the distances are similar to that between benzene and these cations.[28,29] But, unlike cation−benzene systems, in which the interaction distances between a cation and six carbon atoms are identical, the cations are always closer to heteroatom(s) than to carbon atom(s). This may result from much more negative charge on the heteroatom(s) than on carbon in a nucleobase, leading to stronger electrostatic interaction between M^{n+} and heteroatom-(s), resulting in the shorter binding distance.

The binding energy (ΔE), binding enthalpy (ΔH), and change of free energy (ΔG) during the complexation are summarized in Table 1. The cation−π binding strengths are very strong in comparison with the common intermolecular interaction, e.g., hydrogen bonding that is normally no stronger than −20 kcal/mol. The ΔH values of Be^{2+}, Mg^{2+}, Ca^{2+} and Li^+ with nucleobases are −223.2 to −187.8, −105.9 to −81.4, −80.9 to −49.3, and −29.3 to −16.9 kcal/mol, respectively, almost as strong as the binding between benzene and these cations.[28,29] Among them, beryllium complexes have the strongest binding strength while lithium complexes have the weakest. In terms of binding enthalpies, the interaction between nucleobases and Be^{2+} or Mg^{2+} is more likely to be a chemical bond than the usual intermolecular interaction. We proposed to name such a strong interaction cation−π bonding, which also exists in the complexes formed by other aromatics and alkaline earth metal cations.[28−30] Overall, according to the optimized geometries and calculated thermodynamic parameters, we can conclude that nucleobases are capable of forming cation−π or cation−π-like complexes with metal cations.

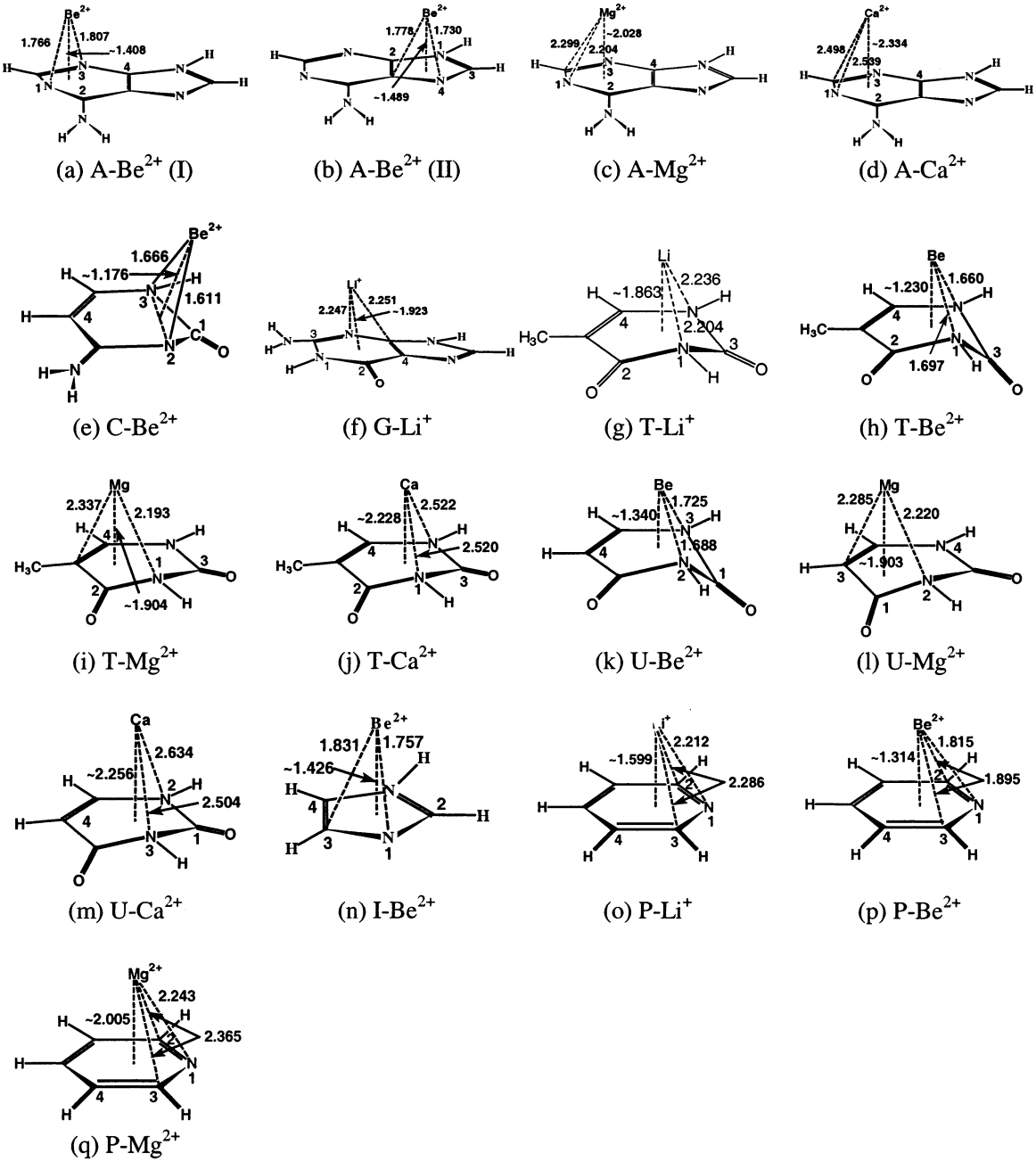

Figure 2. The optimized geometries of the cation−π complexes at the DFT/6-311++G(d,p) level.

Table 1 also shows that Be^{2+} binds to cytosine more strongly than to thymine by ~10% (Figure 2e,h). This could be attributed to richer electrons being located on the cytosine ring than on thymine. For instance, the sum of the total Mulliken charge of the 6 ring atoms of free cytosine and thymine at the DFT/6-311++G(d,p) level are −0.561 and −0.065, respectively. Therefore, Be^{2+} could obtain more electrons from cytosine than from thymine. This supposition is supported by the Mulliken charge of beryllium in the two corresponding complexes. In the former complex, beryllium owns a positive charge of 0.527 atomic units, while in the latter, it is 0.564. The case is similar in the Be^{2+}−uracil complex, in which the binding is ~15% weaker than that in the Be^{2+}−cytocine complex.

3.2. Cation−Heteroatom Complexes. *Lithium Ion Complexes with Nucleobases.* Thirteen optimized structures of Li^+−heteroatom complexes were obtained, which are very similar to what was reported by Russo (refer to Figure 1 and Table 1 in the Supporting Information for calculated geometries and energetics). A similar conclusion to that of Russo's group was found in that the five-membered ring is a favorable binding pattern for bidentate cation−heteroatom complexes, and that the bidentate complex is more stable than the unidentate complex. The experimental binding strength between Li^+ and cytosine is −55.4 kcal/mol,[13] while our predicted ΔH values are −68.5 and 47.3 kcal/mol for two possible binding patterns. Furthermore, Russo et al. showed that one of the cytosine tautomers has a binding affinity of 53.80 kcal/mol to Li^+, which is very close to the experimental result. Another possible explanation is that the experimental result could be based on an average of the two ΔH values of −68.5 and 47.3 kcal/mol. Therefore, more work is needed to clarify whether the experimental result is an average of the two different binding patterns or a tautomer's binding. The case is similar to the complex formed by guanine and Li^+.

Sodium Ion Complexes with Nucleobases. Twelve optimized structures formed by Na^+ with nucleobases were obtained

TABLE 1: The Calculated Parameters of Cation−π Complexes at the B3LYP/6-311++G(d,p) Level (Torsion in deg, Distance in Å, Others in kcal/mol)

geometry	$T_{1-2-3-4}$	E_d	R	ΔE	ΔH	ΔG
Figure 2a, A−Be^{2+}(I)	153.7	18.07	1.408	−223.92	−223.17	−213.63
Figure 2b, A−Be^{2+}(II)	166.0	14.11	1.489	−210.28	−209.79	−200.56
Figure 2c, A−Mg^{2+}	166.3	9.21	2.028	−114.88	−114.65	−105.95
Figure 2d, A−Ca^{2+}	175.3	4.65	2.334	−81.39	−80.94	−72.42
Figure 2e, C−Be^{2+}	112.1	51.12	(1.176)[a]	−221.99	−220.49	−212.02
Figure 2f, G−Li^+	163.6	3.83	1.923	−26.39	−26.04	−19.09
Figure 2g, T−Li^+	149.9	5.84	(1.863)[a]	−17.35	−16.95	−9.56
Figure 2h, T−Be^{2+}	116.9	42.44	(1.230)[a]	−200.20	−200.48	−191.76
Figure 2i, T−Mg^{2+}	134.5	21.98	(1.904)[a]	−93.64	−93.84	−85.61
Figure 2j, T−Ca^{2+}	141.8	12.82	(2.228)[a]	−55.94	−56.05	−48.04
Figure 2k, U−Be^{2+}	132.8	40.98	(1.340)[a]	−187.56	−187.87	−179.17
Figure 2l, U−Mg^{2+}	134.1	22.89	(1.903)[a]	−89.48	−89.54	−81.33
Figure 2m, U−Ca^{2+}	146.7	12.14	(2.256)[a]	−49.31	−49.30	−41.59
Figure 2n, I−Be^{2+}	176.1	3.70	1.426	−197.57	−196.75	−187.97
Figure 2o, P−Li^+	176.8	0.46	1.599	−29.10	−28.29	−20.61
Figure 2p, P−Be^{2+}	173.1	4.76	1.314	−201.24	−200.88	−192.04
Figure 2q, P−Mg^{2+}	174.0	2.27	2.005	−98.36	−98.04	−90.08

[a] The interaction distance is only roughly the perpendicular distance between the cation and the base plane due to the significant ring distortion in their complexes.

TABLE 2: The Calculated Thermodynamic Parameters of Na^+−Nucleobase Cation−Heteroatom Complexes at theB3LYP/6-311++G(d,p) Level (Distance in Å, Others in kcal/mol)

geometry	ΔE	ΔH	ΔG	R	R[g]	ΔH(298K)[g]
Figure 3a, A−Na^+(I)	−34.30	−33.46	−25.02	2.347, 2.477	2.30[a]	−25.6,[a] −41.1,[b] −31.3,[c] −29.7[d]
Figure 3b, A−Na^+(II)	−33.38	−32.56	−24.31	2.352, 2.484		
Figure 3c, A−Na^+(III)	−31.32	−30.69	−23.15	2.282		
Figure 3d, C−Na^+	−53.10	−51.42	−43.98	2.219, 2.475		42.3,[b] −50.1[d]
Figure 3e, G−Na^+(I)	−57.32	−56.57	−49.24	2.281, 2.395	2.26, 2.41[a]	−56.8,[a] −43.5,[b] −54.4[d]
Figure 3f, G−Na^+(II)	−24.69	−24.15	−17.59	2.352, 2.447		
Figure 3g, T−Na^+(I)	−36.92	−36.22	−29.08	2.101		−34.4,[b] −34.2[d]
Figure 3h, T−Na^+(II)	−33.62	−33.61	−25.74	2.106		−33.2[c]
Figure 3i, U−Na^+(I)	−37.11	−36.42	−29.35	2.104		−33.7,[b] −31.3,[c] −34.1[d]
Figure 3j, U−Na^+(II)	−33.04	−32.45	−25.47	2.112		
Figure 3k, I−Na^+	−38.09	−37.24	−30.17	2.276	2.312[d]	−33.4,[e] −34.9[c]
Figure 3l, P−Na^+	−33.18	−32.41	−25.44	2.304		−30.3(0.7)[f]

[a] MP2 calculated result from ref 14. [b] Experimental result from ref 13. [c] Experimental result from ref 12. [d] B3LYP/6-311+G(2df,2p) result from ref 16. [e] Experimental result from ref 32. [f] Experimental result from ref 31. [g] Reference result.

(Figure 3), five of them being very similar to Russo's result as indicated in parts a, d, e, g, and i of Figure 3. The predicted thermochemical parameters and interaction distance, *R*, are listed in Table 2. In brief, the geometrical characteristic of these complexes is very similar to that of the complexes formed between Li^+ and nucleobases. However, only one stable structure formed by cytosine and Na^+ was obtained, while Li^+ has two. On the average, the binding between Na^+ and nucleobases is ∼15 kcal/mol weaker than that between Li^+ and nucleobases. This change can be derived from its interaction distance, which is longer by ∼0.4 Å than the corresponding distance in the Li^+ complex.

The MP2 predicted ΔE of the Na^+−adenine complex is −25.6 kcal/mol,[14] while our B3LYP/6-311++G(d,p) ΔH values are −33.46, −32.56, and −30.69 kcal/mol for A−Na^+(I), A−Na^+(II), and A−Na^+(III), respectively. The experimental result was reported as −41.1 kcal/mol by Cerda et al.[13] and −31.3 kcal/mol by Amunugama et al.[12] The latter is in line with our calculated results, indicating that all three binding patterns are possible. For the complexes formed by Na^+ with thymine and uracil, or with imidazole and pyridine, our predicted binding enthalpies are very close to experimental data with a difference of less than 3 kcal/mol.[12,13,16,31,32] However, our calculated ΔH for C−Na^+(I) is −51.42 kcal/mol, while the experimental value is −42.3 kcal/mol, which is very close to the binding affinity of one cytosine tautomer to Na^+.[13,16] Regarding the binding strength of Na^+ to guanine, the case is very similar to Li^+ in that while the experimental result is −43.5 kcal/mol indicating close affinity of Na^+ to a guanine tautomer,[13,16] it is also proximate to an average value of our calculated ΔH values for the structures G−Na^+(I) and G−Na^+(II).

Potassium Ion Complexes with Nucleobases. Geometrical optimization found 12 optimized structures of K^+−heteroatom complexes (Figure 3), 5 of them being similar to Russo's result.[16] Table 3 listed the predicted values of ΔE, ΔH, ΔG, and *R*. It is indicative from Table 3 that the predicted binding enthalpies are in general weaker than that of Na^+−nucleobase complexes by ∼11 kcal/mol, and the interaction distances are in general longer than those of Na^+−nucleobase complexes by ∼0.4 Å.

The predicted ΔH for the complex of C−K^+(I) is −39.03 kcal/mol, which is far from the experimental result of −26.3 kcal/mol.[13] The experimental binding strength for the K^+−guanine complex is −28.0 kcal/mol,[13] which is very close to the average value of the ΔH of our two predicted structures of G−K^+(I) and G−K^+(II), −43.38 and −13.11 kcal/mol, respectively. Russo et al. suggested that the difference between experimental and predicted binding strengths can be attributed to the tautomerization of nucleobases.[16] The predicted ΔH values for the rest of the potassium complexes in Figure 3 are in good agreement with the experimental data with a difference mostly less than 2 kcal/mol (Table 3).

Meanwhile, although the two possible binding sites in thymine or in uracil are very similar, the binding patterns in T−M^+(I) and U−M^+(I) are more stable than that in T−M^+(II) and

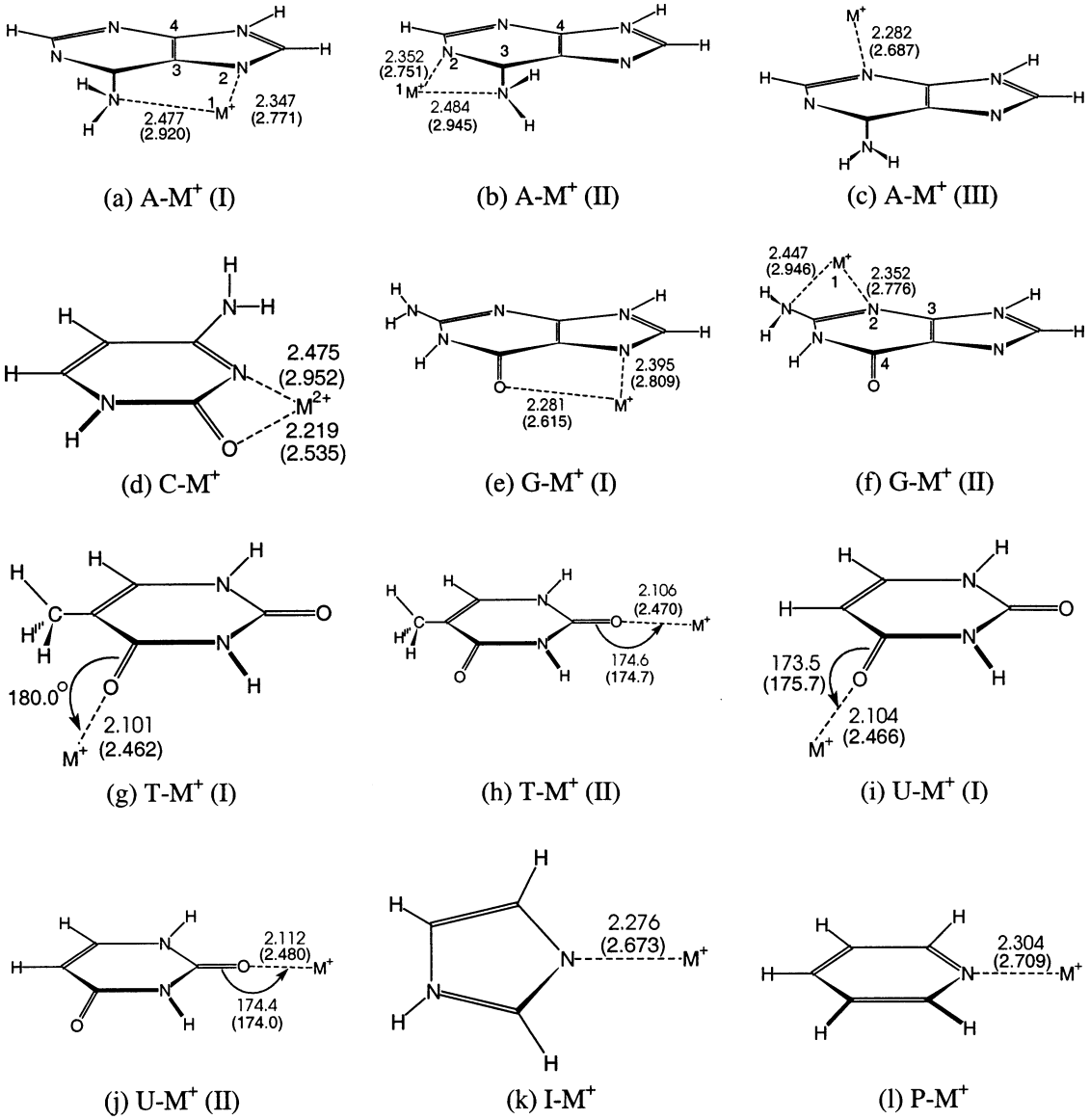

Figure 3. The optimized complexes of nucleobase complexes with Na^+ and K^+ at the B3LYP/6-311++G** level. The distances are in angstroms. Data in parentheses are for K^+.

TABLE 3: The Calculated Thermodynamic Parameters of K^+−Nucleobase Cation−Heteroatom Complexes at theB3LYP/ 6-311++G(d,p) Level (Distance in Å, Others in kcal/mol)

geometry	ΔE	ΔH	ΔG	R	R^e	ΔH(298K)^e
Figure 3a, A−K^+(I)	−21.95	−21.19	−13.20	2.771, 2.920	2.79[a]	−14.6,[a] −25.3,[b] −18.2[c]
Figure 3b, A−K^+(II)	−22.17	−21.40	−13.63	2.751, 2.945		
Figure 3c, A−K^+(III)	−21.02	−20.31	−13.52	2.687		
Figure 3d, C−K^+	−40.52	−39.03	−32.25	2.535, 2.952		−26.3,[b] −37.5[c]
Figure 3e, G−K^+(I)	−44.00	−43.38	−36.26	2.615, 2.809	2.67, 2.86[a]	−40.7,[a] −28.0,[b] −42.2[c]
Figure 3f, G−K^+(II)	−13.59	−13.11	−6.27	2.776, 2.946		
Figure 3g, T−K^+(I)	−27.30	−26.74	−20.01	2.462		−24.3,[b] −25.0[c]
Figure 3h, T−K^+(II)	−25.58	−25.11	−18.42	2.470		
Figure 3i, U−K^+(I)	−27.61	−27.03	−20.34	2.466		−24.1,[b] −25.3[c]
Figure 3j, U−K^+(II)	−23.92	−23.45	−16.84	2.480		
Figure 3k, I−K^+	−27.46	−27.75	−20.20	2.673		
Figure 3*l*, P−K^+	−23.10	−22.47	−16.04	2.709		−21.6(0.9)[d]

[a] MP2 calculation result from ref 14. [b] Experimental result from ref 13. [c] B3LYP/6-311+G(2df,2p) result from ref 16. [d] Experimental result from ref 31. [e] Reference result.

U−M^+(II). Our calculated atomic charges showed that the two oxygen atoms in thymine or uracil are almost charged equally, while the hydrogen atoms attached to carbon atoms are less positively charged than the hydrogen atoms attached to nitrogen atoms. Thus, the repulsion between M^+ and the hydrogen atom attached to the carbon atom should be weaker than that for the hydrogen atom attached to nitrogen. This might be the reason the binding in T−M^+(I) and U−M^+(I) is stronger. Furthermore, the structural unit C═O···M^+, with exception to T−M^+(I), is not linear and is slightly bent by 4−6°. The cause could be due to the different charge distributions as well.

All the M^+−heteroatom complexes have planar structure,

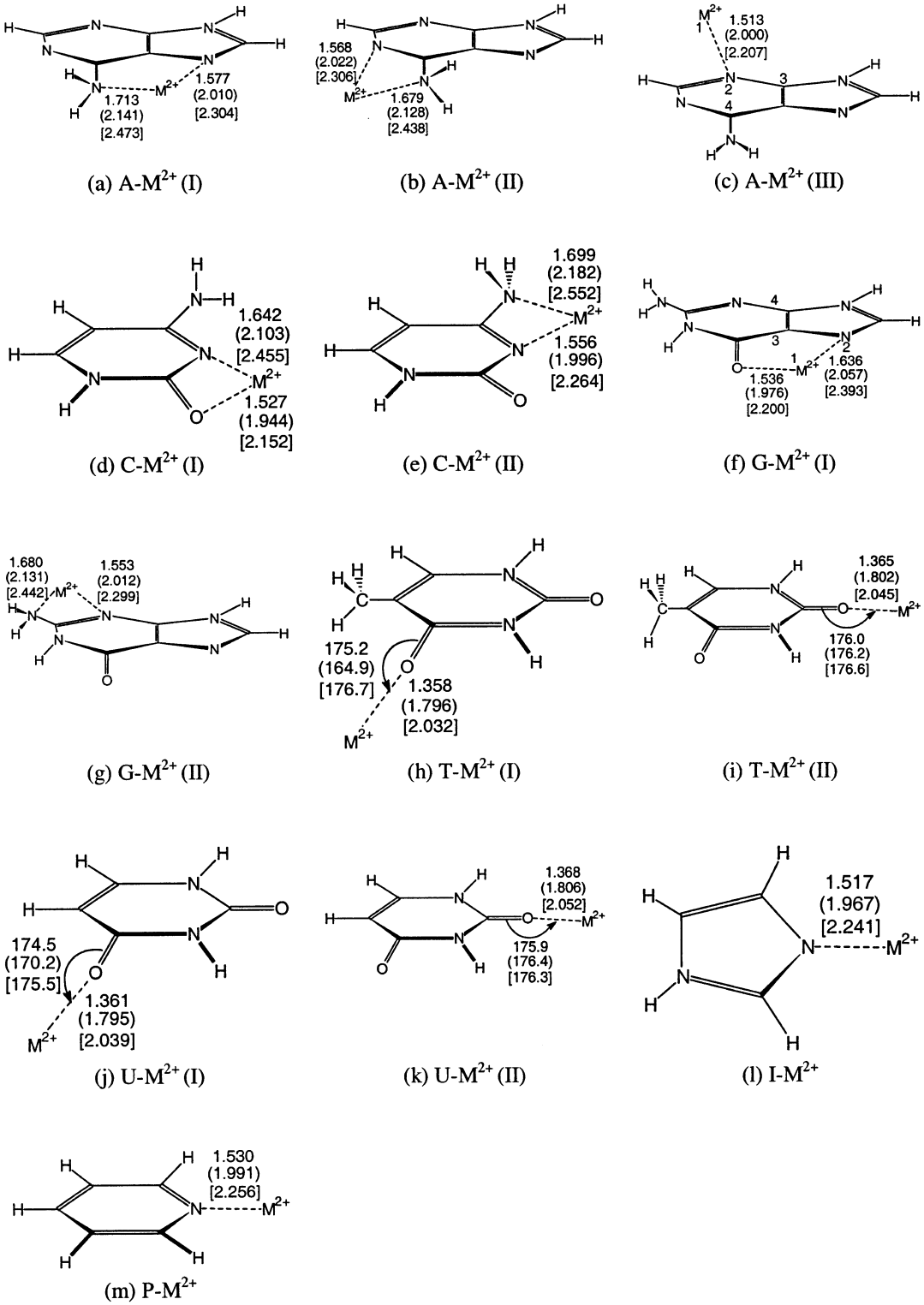

Figure 4. The optimized structures of nucleobases with alkali earth metal cations at the B3LYP/6-311++G** level. The distances are in angstroms. Data in parentheses are for Mg^{2+}, and data in brackets are for Ca^{2+}.

with the exception of the complex C−Li^+(II) and the complexes of A−K^+(I, II) and G−K^+(II) with torsion angles, $T_{1-2-3-4}$, of 163.2°, 149.0°, 143.1°, and 117.6°, respectively. To check the reasonableness of these structures, all the ring atoms and Li^+ were reset to the same plane, then B3LYP/6-311++G(d,p) was directly employed to fully optimize this new initial structure. The same structure as before was obtained, suggesting that noncoplanar interaction can also be a possible binding pattern.

Beryllium Ion Complexes with Nucleobases. Thirteen optimized structures of Be^{2+}−heteroatom complexes were obtained (Figure 4). Table 4 summarizes the calculated thermodynamic parameters and interaction distances. Although beryllium and lithium are in the same row in the periodic table, the predicted binding strength (ΔH) for Be^{2+} complexes is stronger than that for Li^+ complexes by more than 150 kcal/mol. And the interaction distances in the Be^{2+} complexes are shorter by ∼0.4 Å than the corresponding Li^+ complexes. These suggest that the positive charge and size of a cation are vital for its binding with nucleobases. Noncoplanarity was also found in A−Be^{2+}(III) and G−Be^{2+}(I) with the torsions, $T_{1-2-3-4}$, of 168.2° and 170°,

TABLE 4: The Calculated Thermodynamic Parameters of Be^{2+}−Nucleobase Cation−Heteroatom Complexes at the B3LYP/6-311++G(d,p) Level (Distance in Å, Others in kcal/mol)

geometry	ΔE	ΔH	ΔG	R
Figure 4a, A−Be^{2+}(I)	−281.17	−279.30	−269.36	1.577, 1.713
Figure 4b, A−Be^{2+}(II)	−276.67	−274.77	−264.98	1.568, 1.679
Figure 4c, A−Be^{2+}(III)	−237.06	−236.12	−227.63	1.513
Figure 4d, C−Be^{2+}(I)	−297.95	−294.99	−285.91	1.527, 1.642
Figure 4e, A−Be^{2+}(II)	−272.35	−269.47	−260.60	1.556, 1.699
Figure 4f, G−Be^{2+}(I)	−319.19	−317.03	−307.86	1.536, 1.636
Figure 4g, G−Be^{2+}(II)	−257.93	−256.67	−248.13	1.553, 1.680
Figure 4h, T−Be^{2+}(I)	−243.64	−242.70	−233.82	1.538
Figure 4i, T−Be^{2+}(II)	−232.31	−231.54	−222.65	1.365
Figure 4j, U−Be^{2+}(I)	−241.31	−239.70	−231.57	1.361
Figure 4k, U−Be^{2+}(II)	−226.50	−225.39	−217.57	1.368
Figure 4*l*, I−Be^{2+}	−229.56	−228.01	−219.85	1.517
Figure 4m, P−Be^{2+}	−220.73	−219.48	−211.68	1.530

respectively. On the other hand, similar to M^+ complexes of thymine and uracil, the C═O···Be^{2+} unit was also found to be a nonlinear structure in the T−Be^{2+} and U−Be^{2+} complexes.

The binding between Be^{2+} and nucleobases is always very strong (at least −219 kcal/mol). The strongest binding, which is −317 kcal/mol, was found in G−Be^{2+}(I). Taking into account the short interaction distance, this binding might be considered as a chemical bonding instead of an usual intermolecular interaction. To date, no experimental result for the Be^{2+}−nucleobase complexes has been reported, hence, no comparison can be made between the experimental and our predicted results.

Magnesium Ion Complexes with Nucleobases. Figure 4 and Table 5 show the 13 optimized structures of Mg^{2+}−heteroatom complexes and the calculated ΔE, ΔH, ΔG, and R values. In comparison with beryllium complexes, the binding in Mg^{2+}−heteroatom complexes is weaker by ∼100 kcal/mol. And the binding distance in the Mg^{2+} complexes is longer by ∼0.4 Å than that in Be^{2+} complexes. Similar to Be^{2+}−adenine complexes, the unidentate complex of Mg^{2+} with adenine is not a planar structure either. The torsion, $T_{1-2-3-4}$ in the complex A−Mg^{2+}(III), is 153.5°. Likewise, the unit C═O···Mg^{2+} in all thymine and uracil complexes is not linear either. Unlike G−Be^{2+} complexes, the G−Mg^{2+} complexes are planar structures. The MP2 binding strength calculated by Burda et al. is −122 kcal/mol. Our calculated strongest binding enthalpy is −161.6 kcal/mol. The difference is as large as 41 kcal/mol, which might result from their optimization that is limited to the interaction between Mg^{2+} and N7 of adenine.[14] Indeed, their designed initial structure is similar to A−Mg^{2+}(III), with a difference of about 14 kcal/mol.

Calcium Ion Complexes with Nucleobases. As shown in Figure 4, 13 optimized structures were recorded. The calculated thermodynamic parameters and interaction distances were shown in Table 6. Comparing Table 6 with Tables 4 and 5, it was observed that the binding between Ca^{2+} and nucleobases is the weakest. The interaction distances in the Ca^{2+} complexes are as long as 2.03−2.26 Å, longer than the corresponding Mg^{2+} complexes by ∼0.2 Å. However, in comparison with the alkali metal cation complexes, the binding strength (ΔH) in calcium complexes is still stronger although the interaction distances in Li^+ complexes, 1.72 to 1.92 Å, are much shorter than that in Ca^{2+} complexes. This result demonstrates that the positive charge of a cation is the dominant factor affecting the binding strength between a metal cation and nucleobases.

TABLE 5: The Calculated Thermodynamic Parameters of Mg^{2+}−Nucleobase Cation−Heteroatom Complexes at the B3LYP/6-311++G(d,p) Level (Distance in Å, Others in kcal/mol)

geometry	ΔE	ΔH	ΔG	R	R^b	ΔH(298K)^b
Figure 4a, A−Mg^{2+}(I)	−164.78	−163.61	−153.94	2.010, 2.141	1.95[a]	−122.3[a]
Figure 4b, A−Mg^{2+}(II)	−161.30	−160.22	−150.72	2.022, 2.128		
Figure 4c, A−Mg^{2+}(III)	−137.13	−136.68	−128.34	2.000		
Figure 4d, C−Mg^{2+}(I)	−184.58	−182.42	−173.64	1.944, 2.103		
Figure 4e, C−Mg^{2+}(II)	−158.70	−156.74	−148.22	1.996, 2.182		
Figure 4f, G−Mg^{2+}(I)	−201.67	−200.40	−191.25	1.967, 2.057	1.94, 2.06[a]	−212.6[a]
Figure 4g, G−Mg^{2+}(II)	−140.61	−140.06	−131.65	2.012, 2.131		
Figure 4h, T−Mg^{2+}(I)	−139.36	−138.75	−131.92	1.796		
Figure 4i, T−Mg^{2+}(II)	−131.15	−131.26	−122.65	1.802		
Figure 4j, U−Mg^{2+}(I)	−137.94	−137.11	−129.40	1.795		
Figure 4k, U−Mg^{2+}(II)	−127.04	−126.59	−119.12	1.806		
Figure 4*l*, I−Mg^{2+}	−136.66	−135.60	−127.70	1.967		
Figure 4m, P−Mg^{2+}	−129.04	−128.21	−120.52	1.991		

[a] MP2 calculation result from ref 14. [b] Reference result.

TABLE 6: The Calculated Parameters of Ca^{2+}−Nucleobase Cation−Heteroatom Complexes at the B3LYP/6-311++G(d,p) Level (Distance in Å, Others in kcal/mol)

geometry	ΔE	ΔH	ΔG	R	R^c	ΔH(298K)^c
Figure 4a, A−Ca^{2+}(I)	−111.65	−110.76	−101.76	2.304, 2.473	2.38[a]	−66.8[a]
Figure 4b, A−Ca^{2+}(II)	−110.67	−109.80	−100.96	2.306, 2.435		
Figure 4c, A−Ca^{2+}(III)	−94.18	−93.86	−85.82	2.207		
Figure 4d, C−Ca^{2+}(I)	−138.85	−136.88	−128.58	2.152, 2.455		
Figure 4e, C−Ca^{2+}(II)	−111.12	−108.99	−101.53	2.264, 2.552		
Figure 4f, G−Ca^{2+}(I)	−151.36	−150.38	−141.68	2.200, 2.393	2.31, 2.48,[ab]	−137.0[a]
Figure 4g, G−Ca^{2+}(II)	−91.98	−91.58	−84.00	2.299, 2.442		
Figure 4h, T−Ca^{2+}(I)	−99.36	−99.54	−61.97	2.045		
Figure 4i, T−Ca^{2+}(II)	−105.89	−105.77	−68.04	2.032		
Figure 4j, U−Ca^{2+}(I)	−106.07	−105.33	−97.46	2.039		
Figure 4k, A−Ca^{2+}(II)	−95.71	−92.26	−87.58	2.052		
Figure 4*l*, I−Ca^{2+}	−96.88	−96.00	−88.58	2.241		
Figure 4m, P−Ca^{2+}	−89.22	−88.58	−81.67	2.256		

[a] The MP2 calculation result from ref 14. [b] Two different binding distances generated from all−electron calculation and pseudopotential calculation, respectively. [c] Reference result.

TABLE 7: The Total Atomic Charges (Q_M/e) of the Cations in Its Nucleobase Complexes

cation−π	QM/e	base−Na^+	Q_M/e	base−K^+	Q_M/e	base−Be^{2+}	Q_M/e	base−Mg^{2+}	Q_M/e	base−Ca^{2+}	Q_M/e
Figure 2a, A−Be^{2+}(I)	0.575	Figure 3a, A−Na^+(I)	0.815	Figure 3a, A−K^+(I)	0.949	Figure 4a, A−Be^{2+}(I)	0.366	Figure 4a, A−Mg^{2+}(I)	1.135	Figure 4a, A−Ca^{2+}(I)	1.494
Figure 2b, A−Be^{2+}(II)	0.585	Figure 3b, A−Na^+(II)	0.789	Figure 3b, A−K^+(II)	0.951	Figure 4b, A−Be^{2+}(II)	0.400	Figure 4b, A−Mg^{2+}(II)	1.070	Figure 4b, A−Ca^{2+}(II)	1.356
Figure 2c, A−Mg^{2+}	0.989	Figure 3c, A−Na^+(III)	0.863	Figure 3c, A−K^+(III)	0.963	Figure 4c, A−Be^{2+}(III)	0.539	Figure 4c, A−Mg^{2+}(III)	1.176	Figure 4c, A−Ca^{2+}(III)	1.521
Figure 2d, A−Ca^{2+}	1.397	Figure 3d, C−Na^+	0.740	Figure 3d, C−K^+	0.938	Figure 4d, C−Be^{2+}(I)	0.473	Figure 4d, C−Mg^{2+}(I)	1.147	Figure 4d, C−Ca^{2+}(I)	1.474
Figure 2e, C−Be^{2+}	0.527	Figure 3e, G−Na^+(I)	0.745	Figure 3e, G−K^+(I)	0.953	Figure 4e, C−Be^{2+}(II)	0.648	Figure 4e, C−Mg^{2+}(II)	1.228	Figure 4e, C−Ca^{2+}(II)	1.571
Figure 2f, G−Li^+	0.645	Figure 3f, G−Na^+(II)	0.853	Figure 3f, G−K^+(II)	0.955	Figure 4f, G−Be^{2+}(I)	0.388	Figure 4f, G−Mg^{2+}(I)	1.103	Figure 4f, G−Ca^{2+}(I)	1.466
Figure 2g, T−Li^+	0.643	Figure 3g, T−Na^+(I)	0.947	Figure 3g, T−K^+(I)	0.975	Figure 4g, G−Be^{2+}(II)	0.365	Figure 4g, G−Mg^{2+}(II)	1.165	Figure 4g, G−Ca^{2+}(II)	1.534
Figure 2h, T−Be^{2+}	0.564	Figure 3h, T−Na^+(II)	0.964	Figure 3h, T−K^+(II)	0.978	Figure 4h, T−Be^{2+}(I)	0.688	Figure 4h, T−Mg^{2+}(I)	1.392	Figure 4h, T−Ca^{2+}(I)	1.669
Figure 2i, T−Mg^{2+}	1.042	Figure 3i, U−Na^+(I)	0.963	Figure 3i, U−K^+(I)	0.978	Figure 4i, T−Be^{2+}(II)	0.733	Figure 4i, T−Mg^{2+}(II)	1.410	Figure 4i, T−Ca^{2+}(II)	1.699
Figure 2j, T−Ca^{2+}	1.562	Figure 3j, U−Na^+(II)	0.966	Figure 3j, U−K^+(II)	0.979	Figure 4j, U−Be^{2+}(I)	0.746	Figure 4j, U−Mg^{2+}(I)	1.422	Figure 4j, U−Ca^{2+}(I)	1.693
Figure 2k, U−Be^{2+}	0.627	Figure 3k, I−Na^+	0.920	Figure 3k, I−K^+	0.980	Figure 4k, U−Be^{2+}(II)	0.741	Figure 4k, U−Mg^{2+}(II)	1.426	Figure 4k, A−Ca^{2+}(II)	1.711
Figure 2*l*, U−Mg^{2+}	1.128	Figure 3*l*, P−Na^+	0.892	Figure 3*l*, P−K^+	0.971	Figure 4*l*, I−Be^{2+}	0.668	Figure 4*l*, I−Mg^{2+}	1.330	Figure 4*l*, I−Ca^{2+}	1.681
Figure 2m, U−Ca^{2+}	1.620					Figure 4m, P−Be^{2+}	0.856	Figure 4m, P−Mg^{2+}	1.416	Figure 4m, P−Ca^{2+}	1.655
Figure 2n, I−Be^{2+}	0.644										
Figure 2o, P−Li^+	0.457										
Figure 2p, P−Be^{2+}	0.641										
Figure 2q, P−Mg^{2+}	1.041										

3.3. Charge Transfer and Molecular Orbital Interaction. Each complex formed by a cation with a nucleobase was divided into two parts as cation and nucleobase. Table 7 summarized the Mulliken charges located on these two parts. The data suggested that charge transfer takes place during the complexation reaction. The data also demonstrated that the stronger the binding, the more the charge being transferred. On average, the transferred positive charge from metal cation to nucleobase, Q, is in the order of $Q(Be^{2+}) > Q(Mg^{2+}) > Q(Ca^{2+}) > Q(Na^+) > Q(K^+)$. As we know, the LUMO energies of these cations increase in the above order, therefore, the electrons should be easier to transfer from nucleobases to Be^{2+} than to K^+. Hence, more positive charge should be transferred from Be^{2+} to nucleobase than from K^+. Concordantly, this order correlated well with the binding strength between nucleobases and M^{n+}. Therefore, the transferred charge between nucleobases and M^{n+} during complexation could be used as an indicator of the binding strength between the nucleobases and the cations. This observation is very similar to our previous studies.[23,29]

To illustrate the possible orbital interaction between cations and nucleobases, as an example, an orbital analysis was carried out on the cation−π complex U−Mg^{2+} in Figure 2*l*, and on the cation−heteroatom complex U−Mg^{2+}(I) in Figure 4j. The result for the cation−π complex demonstrated that the maximum orbital contribution of Mg^{2+} to the first 10 highest occupied molecular orbitals was found in HOMO, in which the contribution from Mg^{2+} was 7.15%. This contribution is most likely to come from its p_x orbital, 4.54%, followed by its p_y orbital, 1.14%, suggesting that it is the p_x and p_y orbitals, rather than p_z orbital, of the cation Mg^{2+} that interact with the π orbital of the aromatic ring. Therefore, we concluded that the orbital interaction between the metal cation and the nucleobase is mainly a p−π interaction. In the cation−heteroatom complex of U−Mg^{2+}(I), the orbital analysis did not reveal any apparent contribution of the Mg^{2+} orbital to the first 10 highest occupied molecular orbitals (<1%), demonstrating that the cation−heteroatom complex is not involved in the orbital interaction between the cation and the nucleobase.

3.4. Morokuma Decomposition on Binding Energy. As an example, the Morokuma decomposition was performed on the complexes formed by adenine and M^{n+} at the HF/6-31G** level based on HF/6-31G** optimized structures. These results were summarized in Table 8, in which the ES, EX, PL, CT, MIX, and ΔE denote electrostatic, exchange repulsion, polarization, charge transfer, high order coupling, and total binding energies, respectively. Table 8 showed that both ES and PL energies are always favorable to the binding between metal cations and nucleobases. However, the ES is less important to the cation−π binding than to the cation−heteroatom binding. For example, the strongest ES is only −36.14 kcal/mol in the cation−π binding, while it is −162.65 kcal/mol in cation−heteroatom binding. Another observation is that the PL was found to be very important for the cation−π binding, which is significantly affected by the cation's radius. The smaller the size of a cation, the greater the PL. This is expected as these three cations own the same amount of positive charge. For instance, the PL values are −857.15, −503.92, and −46.69 kcal/mol in A−Be^{2+}(I), A−Mg^{2+}(I), and A−Ca^{2+}(I) cation−π complexes, respectively. Furthermore, the EX and MIX were found to be positive. Therefore, they are the main obstruction for the metal cations to bind to nucleobases.

The contribution of CT to cation−π binding was estimated as +184.25, −198.85, and −232.49 kcal/mol for Be^{2+}, Mg^{2+}, and Ca^{2+} to bind to adenine, respectively, suggesting that CT

TABLE 8: Morokuma Decomposition Analysis Results Corrected by BSSE at the HF/6-31G Level**

type	structure	ES	EX	PL	CT	MIX	ΔE
cation$-\pi$	Figure 2a, A$-Be^{2+}$(I)	−27.79	41.43	−857.15	184.25	424.56	−234.69
	Figure 2c, A$-Mg^{2+}$(I)	−36.14	21.46	−503.92	−198.85	599.49	−117.96
	Figure 2d, A$-Ca^{2+}$(I)	−29.39	16.30	−46.69	−232.49	224.60	−67.66
cation−heteroatom	Figure 3a, A$-Na^{+}$(I)	−42.37	11.40	−16.27	−2.74	3.90	−46.08
	Figure 3a, A$-K^{+}$(I)	−25.93	7.32	−8.86	−2.36	1.78	−28.04
	Figure 4a, A$-Be^{2+}$(I)	−162.65	68.64	−542.31	−206.17	539.70	−302.78
	Figure 4a, A$-Mg^{2+}$(I)	−125.12	43.43	−330.48	−100.38	335.80	−176.77
	Figure 4a, A$-Ca^{2+}$(I)	−91.57	32.69	−63.85	−10.47	18.71	−114.49

is more beneficial to the binding of Ca^{2+} with adenine than that of Be^{2+} and Mg^{2+}. We recalculated these values, but the result remained the same. Thereupon we deduced that this result could be related to the different deformation of adenine planar ring structures in different systems. Indeed, the deformation in Be^{2+}−adenine is significant ($T = 153.7°$, Figure 2a), but it is minute in the case of Ca^{2+}−adenine ($T = 175.3°$, Figure 2d). The good planarity of the adenine ring structure in A$-Ca^{2+}$(I) allows its π electrons to be transferred to Ca^{2+} easily, therefore giving greater contribution to CT energy.

4. Conclusions

On the basis of the B3LYP/6-311++G(d,p) calculation and Morokuma decomposition results, the interaction between alkaline or alkaline earth metal cations and nucleobases could be summarized as follows.

(1) Both cation$-\pi$ and cation−heteroatom binding are possible between metal cations and nucleobases, due to the planar structures of nucleobases. While only the alkaline earth cations and lithium ion can form cation$-\pi$ complexes with nucleobases, all the alkaline or alkaline earth metal cations can form cation−heteroatom complexes. The same cation could form more than one cation−heteroatom complex with the same nucleobase due to more than one possible binding site in a nucleobase. Therefore, the interaction pattern might be different in different situations.

(2) The distortion of the planar ring structure of nucleobase takes place during its cation$-\pi$ binding with metal cations, especially in the cases of cytosine, thymine, and uracil, which could probably be attributed to the existence of the carbonyl structure. The stronger capability of adenine and guanine to keep their planar ring structures in their complexes might be accounted for by their condensed ring structures. The distortion energies imply that the aromaticity of cytosine, thymine, and uracil is more or less destroyed. Therefore, a cation$-\pi$-like complex might be a better term for these complexes.

(3) The interaction distance between a cation and the ring plane of a nucleobase in their cation$-\pi$ or cation$-\pi$-like complex is rather short, ranging from ∼1.3 to ∼2.3 Å. The ΔH of the complexation reaction ranges from −16.95 to −223.17 kcal/mol, indicating that cation$-\pi$ or cation$-\pi$-like binding are as strong as the binding between benzene and these cations.

(4) The cation−heteroatom interaction, in which a cation directly binds to the heteroatom(s) of the nucleobases and is usually located in the same plane as ring atoms, can be either unidentate or bidentate. But, the bidentate binding, in which a cation is bound to two heteroatoms, was found to be stronger than unidentate binding.

(5) The calculated B3LYP/6-311++G(d,p) ΔH values are in general in good agreement with the reported experimental data. Those determined ΔH values that are different from the calculated values are close to the average of the binding strength of two different isomeric structures formed by the same cation and same base.

(6) While the orbital interaction is significantly involved in cation$-\pi$ binding, no apparent orbital interaction was found in cation−heteroatom interaction.

In conclusion, the interaction between nucleobases and alkaline or alkaline earth metal cations is multiple, flexible, and strong. The hydrogen bonding in a base pair of a nucleic acid could be seriously affected or broken by the interaction, resulting in a change in the bio-functions of a nucleic acid. Therefore, these calculation results might help us to better understand the role of various cations in biological systems and to evaluate their effects in biological processing. The revealed geometrical and thermochemical parameters as well as the calculated total atomic charges are useful for improving the current force field to reproduce such kinds of interactions that are essential in exploring the role of cations in living systems.

Acknowledgment. This work was supported by the State Key Program of Basic Research of China (grant 2002CB512802), the National Natural Science Foundation of China (grants 20372069, 29725203, and 20072042), Shanghai Basic Research Project from the Shanghai Science and Technology Commission (grant 02DJ14070), and the 863 Hi-Tech Program (grants 2001AA235051, 2001AA235071, and 2002AA233011). The quantum chemistry calculations were performed on Power Challenge R10000 at the Network Information Center, Chinese Academy of Sciences, Beijing, P. R. China and on P4 PCs at Singapore Polytechnic, Singapore.

Supporting Information Available: Table giving the calculated thermodynamic parameters of Li^{+}−nucleobase cation−heteratom complexes at the B3LYP/6-311++G(d,p) level and the optimized structures of Li^{+}−nucleopbase complexes at the B3LYP/6-311++G** level. This material is available free of charge via the Internet at http://pubs.acs.org.

References and Notes

(1) Ma Jennifer, C.; Dougherty, D. A. *Chem. Rev.* **1997**, *97*, 1303.
(2) Rulíšek, L.; Havlas, Z. *J. Am. Chem. Soc.* **2000**, *122* (42), 10428.
(3) Kaim, W.; Schwederski, B. *Bioinorganic Chemistry*: *Inorganic Elements in the Chemistry of Life*; John Wiley & Sons: Chichester, UK, 1994.
(4) Lippard, S. J.; Berg, J. M. *Principles of Bioinorganic Chemistry*; University Science Books: Mill Balley, CA, 1994.
(5) Del Bene, J. E. *J. Phys. Chem.* **1984**, *88*, 5927.
(6) Basch, H.; Krauss, M.; Stevens, W. J. *J. Am. Chem. Soc.* **1985**, *107*, 7265.
(7) Lipinski, J. *J. Mol. Struct. (THEOCHEM)* **1989,** *201*, 87.
(8) Hobza, P.; Sandorfy, C. *J. Biomol. Struct. Dyn.* **1985**, *2*, 1245.
(9) Anwander, E. H. S.; Probst, M. M.; Rode, B. M. *Biopolymers* **1990**, *29A*, 757.
(10) Šponer, J.; Sabat, M.; Burda, J. V.; Leszczynski, J.; Hobza, P. *J. Phys. Chem. B* **1999**, *103*, 2528.
(11) Šponer, J.; Burda, J. V.; Sabat, M.; Leszczynski, J.; Hobza, P. *J. Phys. Chem. A* **1998**, *102*, 5951.
(12) Hoyau, S.; Norrman, K.; McMahon, T. B.; Ohanessian, G. *J. Am. Chem. Soc.* **1999**, *121*, 8864.
(13) Cerda, B. A.; Wesdemiotis, C. *J. Am. Chem. Soc.*, **1996**, *118*, 11884. Cerda, B. A.; Hoyau, S.; Ohanessian, G.; Wesdemiotis, C. *J. Am. Chem. Soc.* **1998**, *120*, 2437.

(14) Burda, J. V.; Šponer, J.; Hobza, P. *J. Phys. Chem.* **1996**, *100*, 7250.
(15) Russo, N.; Toscano, M.; Grand, A. *J. Phys. Chem. B* **2001**, *105*, 4735.
(16) Russo, N.; Toscano, M.; Grand, A. *J. Am. Chem. Soc.* **2001**, *123*, 10272.
(17) Felder, C.; Jiang, H. L.; Zhu, W. L.; Chen, K. X.; Silman, I.; Botti, S. A.; Sussman, J. L. *J. Phys. Chem.* **2001**, *105*, 1326.
(18) Parr, R. G.; Yang, W. *Density-functional theory of atoms and molecules*; Oxford University Press: Oxford, UK, 1989.
(19) Becke, A. D. *J. Chem. Phys.* **1993**, *98*, 5648.
(20) Dunbar, R. C. *J. Phys. Chem. A* **2000**, *104*, 8067.
(21) Zhu, W. L.; Jiang, H. L.; Puah, C. M.; Tan, X. J.; Chen, K. X.; Cao, Y.; Ji, R. Y. *J. Chem. Soc., Perkin Trans. 2* **1999**, *11*, 2615.
(22) Peschke, M.; Blades, A. T.; Kebarle, P. *J. Am. Chem. Soc.* **2000**, *122*, 1492.
(23) Zhu, W. L.; Tan, X. J.; Puah, C. M.; Gu, J. D.; Jiang, H. L.; Chen, K. X.; Felder, C. E.; Silman, I.; Sussman, J. L. *J. Phys. Chem. A* **2000**, *104*, 9573.
(24) Peschke, M.; Blades, A. T.; Kebarle, P. *J. Am. Chem. Soc.* **2000**, *122*, 10440.
(25) Kitaura, K.; Morokuma, K. *Int. J. Quantum Chem.* **1976**, *10*, 325.
(26) Frisch, M. J.; Trucks, G. W.; Schlegel, H. B.; Scuseria, G. E.; Robb, M. A.; Cheeseman, J. R.; Zakrzewski, V. G.; Montgomery, J. A., Jr.; Stratmann, R. E.; Burant, J. C.; Dapprich, S.; Millam, J. M.; Daniels, A. D.; Kudin, K. N.; Strain, M. C.; Farkas, O.; Tomasi, J.; Barone, V.; Cossi, M.; Cammi, R.; Mennucci, B.; Pomelli, C.; Adamo, C.; Clifford, S.; Ochterski, J.; Petersson, G. A.; Ayala, P. Y.; Cui, Q.; Morokuma, K.; Malick, D. K.; Rabuck, A. D.; Raghavachari, K.; Foresman, J. B.; Cioslowski, J.; Ortiz, J. V.; Stefanov, B. B.; Liu, G.; Liashenko, A.; Piskorz, P.; Komaromi, I.; Gomperts, R.; Martin, R. L.; Fox, D. J.; Keith, T.; Al-Laham, M. A.; Peng, C. Y.; Nanayakkara, A.; Gonzalez, C.; Challacombe, M.; Gill, P. M. W.; Johnson, B. G.; Chen, W.; Wong, M. W.; Andres, J. L.; Head-Gordon, M.; Replogle, E. S.; Pople, J. A. *Gaussian 98*; Gaussian, Inc.: Pittsburgh, PA, 1998.
(27) Schmidt, M. W.; Baldridge, K. K.; Boatz, J. A.; Elbert, S. T.; Gordon, M. S.; Jensen, J. H.; Koseki, S.; Matsunaga, N.; Nguyen, K. A.; Su, S. J.; Windus, T. L.; Dupuis, M.; Montgomery, J. A. *J. Comput. Chem.*, **1993**, *14*, 1347.
(28) (a) Jiang, H. L.; Zhu, W. L.; Tan, X. J.; Chen, J. Z.; Zhai Y. F.; Liu, D. X.; Zhao, L.; Chen, K. X.; Ji, R. Y. *Acta Chim. Sin.* **1999**, *57*, 860. (b) Nicholas, J. B.; Hay, B. P.; Dixon, D. A. *J. Phys. Chem.* **1999**, *103*, 1394.
(29) Tan, X. J.; Zhu W. L.; Cui, M.; Luo, X. M.; Gu, J. D.; Silman, I.; Sussman, J. L.; Jiang H. L.; Ji, R. Y.; Chen, K. X. *Chem. Phys. Lett.* **2001**, *349*, 113.
(30) (a) Zhu, W. L.; Liu, T.; Shen, J. H.; Luo, X. M.; Tan, X. J.; Puah, C. M.; Jiang, H. L.; Chen, K. X. *Chem. Phys. Lett.* **2002**, *366*, 267. (b) Zhu, W.; Tan, X.; Shen, J.; Luo, X.; Cheng, F.; Puah, C. M.; Ji, R.; Chen, K.; Jiang, H. *J. Phys. Chem. A* **2003**, *107*, 2296.
(31) Amunugama, R.; Rodgers, M. T. *Int. J. Mass Spectrom.* **2000**, *195/196*, 439.
(32) Armentrout, P. B.; Rodgers, M. T. *J. Phys. Chem.* **2000**, *104*, 2238.